Imaging Structural Changes of the Mouse Retina in Retinitis Pigmentosa with Balanced Steady State Free Precession

E. R. Muir¹, B. H. De La Garza¹, and T. Q. Duong¹

¹Research Imaging Institute, University of Texas Health Science Center, San Antonio, TX, United States

INTRODUCTION: The retina consists of highly structured neuronal and synaptic layers and is only about 250 µm thick in rodents, including the choroid (1). The layers of the retina, starting from the vitreous, include the ganglion cell layer, the inner plexiform layer, the inner nuclear layer, the outer plexiform layer, the outer nuclear layer (ONL) which consists of the photoreceptor nuclei, the inner and outer segments (IS/OS) of the photoreceptor cells, and the retinal pigment epithelium (RPE). The choroid, not part of the neural retina, is next to the RPE.

The goal of this study was to develop a high contrast, high resolution, high sensitivity, and fast imaging approach, based on balanced steady state free precession (bSSFP), to resolve different layers of the retina at $42x42x400 \, \mu m$. We applied this approach to investigate a mouse model of retinitis pigmentosa (RP). RP, the most common inherited retinal degeneration, causes photoreceptor death and blindness and affects 1.5 million people worldwide (2). It is characterized by a progressive loss of photoreceptors (ONL and IS/OS) with secondary degeneration of other layers. Different stages of retinal degeneration along with age-matched controls were evaluated with MRI. Comparison was made with histology.

METHODS: The rd10 mouse model of RP on a C57BL/6J background was used, with wild type (WT) C57BL/6J mice used for controls. MRI was done on mice at post natal days 25, 35, and 60 (P25, P35, and P60) (n=32 total). Mice were imaged under \sim 1.1% isoflurane in 30% oxygen and spontaneous breathing conditions. Respiration rate and temperature were monitored and maintained. MRI was performed on a 7T/30cm Bruker scanner with a 150 G/cm gradient and a small surface eye coil. Images were acquired in coronal orientation with bSSFP with FOV=5x5 mm, matrix=120x120 (42x42 μm) zero-filled to 128x128, a single 0.4 mm slice, and TE/TR=3.6/7.2 ms, and oversampling by a factor of 2 in frequency and phase encode directions. Profile analysis was used to create average anatomical profiles of the whole retina for thickness measurement (1). Additionally, higher resolution MRI was tested on mice at P25 using FOV=4.48x4.48x3.2 mm, matrix=128x128x16 (35x35x200 μm) zero-filled to 256x256x16, TE/TR= 3.3/6.5 ms, and oversampling by 2 in frequency and first phase encode directions. Retinal histology was acquired at P25 and P60 to assess anatomical degeneration. Eyes were enucleated, fixed in 10% paraformaldehyde, embedded in paraffin, sectioned at 8 μm, and stained with hematoxylin and eosin. Statistical analysis used Wilcoxon rank-sum test for MRI data and two-way ANOVA with Bonferroni post-hoc for histological data.

RESULTS: bSSFP at 42x42 µm resolved 4 layers in the retina of WT mice, including the choroid. In contrast, bSSFP resolved 2 layers in the retina of rd10 mice (**Figures 1,2**). The thicknesses of the neural retina from MRI (layers 1-3) and histology are shown in **Figure 3**. The rd10 retina was significantly thinner at all ages compared to WT, from MRI and histology. The rd10 retina at P25 was significantly thicker than at P35 and P60 (p<0.01) from MRI and at P60 from histology (p<1E-7). From the histology, outer retinal layers of rd10 mice were thinned at P25; at P60 the outer layers were further degenerated and inner retinal layers were also thinned. The neural retina was thinner measured from MRI compared to histology.

At higher spatial resolution $(35x35x200 \ \mu m)$, bSSFP resolved 6 retinal layers, including the choroid, in WT mice at P25 and 4 layers in rd10 mice at P25 (**Figure 4**). Total neural retinal thickness was not significantly different between the lower and higher resolution MRI.

DISCUSSION: High spatiotemporal resolution, high sensitivity bSSFP MRI detected longitudinal thinning of the retina in the rd10 mouse model of RP. We previously found that bSSFP provided better contrast and SNR in the retina compared to gradient echo sequences (3). The current findings demonstrate the utility of bSSFP in imaging anatomical changes of the retina. Because MRI is non-invasive, provides depth resolution and large field of view, it could be used for longitudinal studies of retinal diseases and monitoring of potential treatments. This approach could complement optical coherence tomography (the only optical imaging approach that has depth resolution) which cannot be readily applied to rodents and has limited FOV. Future studies will further advance spatial resolution, include 3D bSSFP, and incorporate BOLD and blood-flow contrast to bSSFP acquisition.

Reference: 1) Cheng et al, PNAS 2006, 103:17525. 2) Berson, IOVS 1993, 34:1659. 3) Muir et al, ISMRM 2010, Stockholm. Supported in part by R01 EY014211, R01 EY018855, CTSA-017A, VA MERIT.

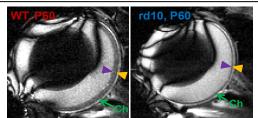


Figure 1. Images of a WT and rd10 mouse eye at P60 at $42x42x400 \mu m$. The green arrow indicates the choroid (Ch). The purple and orange arrowheads indicate the inner and outer boundary of the retina, respectively.

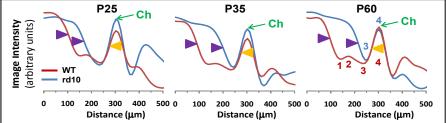


Figure 2. Group-average anatomical profiles from WT and rd10 mice at P25, P 35, and P60 (n are the same as shown in Figure 3). MRI layers are labeled on P60 profiles (1-4 in red for WT mice, 3-4 in blue for rd10). The green arrow indicates the choroid (Ch, layer 4). The purple and orange arrowheads indicate the inner and outer boundary of the retina, respectively.

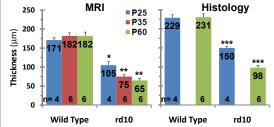


Figure 3. Group-average neural retinal thicknesses from MRI $(42x42x400 \mu m)$ and histology (mean±SD). *p<0.05, **p<0.01, ***p<1E-7 compared to age-matched WT mice.

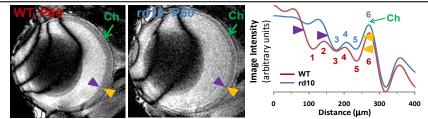


Figure 4. Images and profiles from wild type and rd10 mice at P25 at 35x35x200 μm. MRI layers are labeled 1-6 in red for WT and layers 3-6 in blue for rd10. The green arrow indicates the choroid (Ch, layer 6). The purple and orange arrowheads indicate the inner and outer boundary of the retina, respectively.